6880 *J. Med. Chem.* **2009,** *52,* 6880–6888
DOI: 10.1021/jm901146p

Journal of Medicinal Chemistry Article

Discovery of A Novel Her-1/Her-2 Dual Tyrosine Kinase Inhibitor for the Treatment of Her-1 Selective Inhibitor-Resistant Non-small Cell Lung Cancer

Mi Young Cha,[†,‡] Kwang-Ok Lee,[†] Jong Woo Kim,[†] Chang Gon Lee,[†] Ji Yeon Song,[†] Young Hoon Kim,[†] Gwan Sun Lee,[†] Seung Bum Park,*[,‡,§] and Maeng Sup Kim*[,†]

[†]*Department of Drug Discovery, Hanmi Research Center, 377-1 Yeongcheon-ri, Dongtan-myeon, Hwaseong, Gyeonggi-do, 445-813, Korea,* [‡]*Department of Chemistry, Seoul National University,* [§]*Department of Biophysics and Chemical Biology, Seoul National University, Seoul 151-747, Korea*

Received July 31, 2009

A novel series of (*S*)-1-acryloyl-*N*-[4-(arylamino)-7-(alkoxy)quinazolin-6-yl]pyrrolidine-2-carboxamides were synthesized and evaluated as Her-1/Her-2 dual inhibitors. In contrast to the Her-1 selective inhibitors, our novel compounds are irreversible inhibitors of Her-1 and Her-2 tyrosine kinases with the potential to overcome clinically relevant, mutation-induced drug resistance. The selected compounds (**19c**, **19d**) showed excellent EGFR inhibition activity even toward the T790M mutation of Her-1 tyrosine kinase with excellent selectivity. The excellent pharmacokinetic profiles of these compounds in rats and their robust in vivo efficacy in an A431 xenograft model clearly demonstrate that they merit further investigation as novel therapeutic agents for EGFR-targeting treatment of solid tumors, especially Her-1 selective inhibitor-resistant non-small cell lung cancer.

Introduction

A signaling cascade of epidermal growth factor receptors (EGFRs[a]), which is composed of four members, Her-1 (ErbB-1), Her-2 (neu, ErbB-2), Her-3 (ErbB-3), and Her-4 (ErbB-4), plays a key role in regulating cell proliferation and differentiation in many tissue types.[1−3] Therefore, dysregulation of the EGFR signaling pathway may contribute to malignant transformation, and overexpression of Her-1 and Her-2 is frequently observed in several solid tumors.[4] Accordingly, the EGFR family is a major target of anticancer agents.[5]

Several small-molecule inhibitors of EGFR tyrosine kinases have been developed (see Figure 1).[6] The first class of EGFR-targeting therapeutic agents includes the Her-1 specific inhibitors, **1** (Gefitinib)[7] and **2** (Erlotinib),[8] for treatment of non-small cell lung cancer. However, the drug's resistance to Her-1 specific inhibitors has been clinically observed and has been associated with the T790M mutation of Her-1 tyrosine kinase.[9] The second class includes the Her-1/Her-2 dual inhibitor, **3** (Lapatinib),[10] for treatment of Her-2-positive breast cancer. Because Her-1 tyrosine kinase binds Her-1 or Her-2 tyrosine kinases to form a homo- or heterodimer for the signal transduction in EGFR signaling cascade, Her-1/Her-2 dual inhibition is more effective than just Her-1 inhibition.[11] The third class includes the EGFR irreversible inhibitors, **4** (HKI-272)[12,13] and **5** (CI-1033).[14] Among these classes of EGFR inhibitors, **4** and **5** drew our attention because of their interesting mode of action; that is, inhibition of EGFR tyrosine kinases through irreversible modification of a Cys residue (Cys773 of Her-1 and Cys805 of Her-2) at their respective active sites. It has recently been reported that irreversible inhibition of EGFR tyrosine kinases can be a more advantageous approach because these agents may be able to overcome accumulating resistance toward the reversible inhibitors, such as **1** and **2**, associated with clinically frequent T790M mutation of Her-1 tyrosine kinase in response to drug treatment.[15−19]

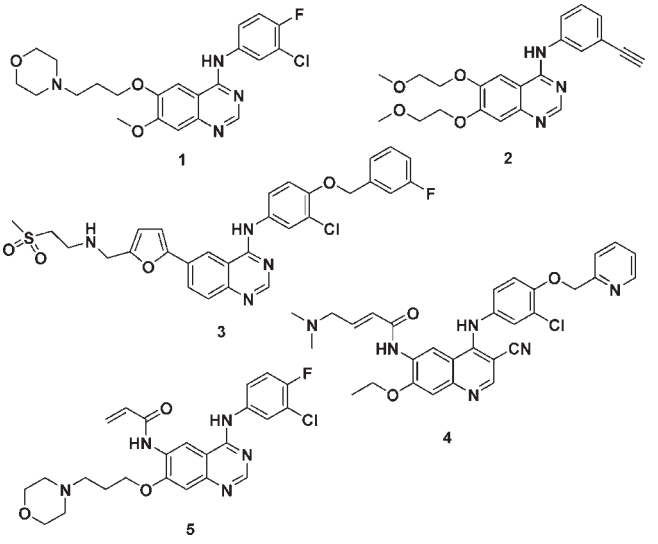

Figure 1. Representative inhibitors of EGFR tyrosine kinases.

Results

Chemical Design and Synthesis. To develop novel EGFR-targeting therapeutic agents with enhanced potency that can

*To whom correspondence should be addressed. Phone: +82-31-3715100 (M.S.K.); +82-2-880-9090 (S.B.P.). Fax: +82-31-3715068 (M.S.K.); +82-2-884-4025 (S.B.P.). E-mail: kims@hanmi.co.kr (M.S.K.); sbpark@snu.ac.kr (S.B.P.).

[a] Abbreviations: Her, human epidermal growth factor receptor; EGFR, epidermal growth factor receptor.

 Published on Web 10/15/2009

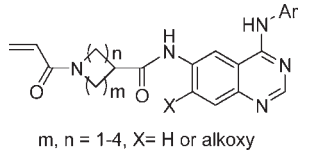

Figure 2. Design of novel Her-1/Her-2 dual inhibitors.

Scheme 1[a]

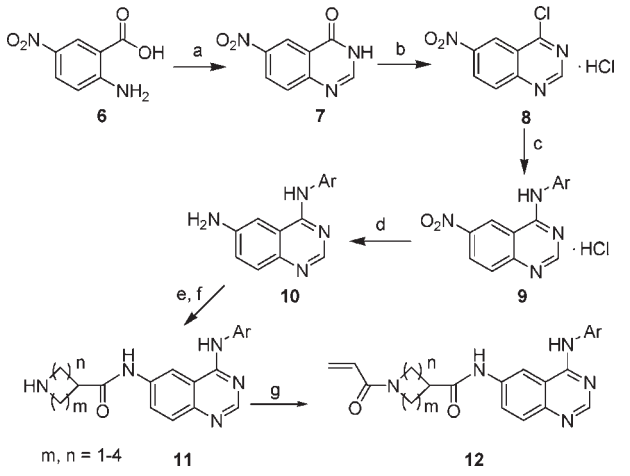

[a] Reagents and conditions: (a) formamide, 170 °C; (b) $SOCl_2$, $POCl_3$, DMF (cat.), reflux; (c) anilines, *i*-PrOH, reflux; (d) Fe, concd HCl (cat.), 50% EtOH, reflux; (e) *N*-Boc-amino acids, EDCI, pyridine, r.t.; (f) TFA, DCM, r.t.; (g) acrylic acid, EDCI, pyridine, THF, 0 °C.

overcome the drug resistance of the Her-1 specific agents, we pursued the synthesis of novel core skeletons inspired by irreversible EGFR inhibitors. As shown in Figure 1, the *N*-acryloyl moiety is commonly shared among the irreversible EGFR inhibitors and is responsible for the covalent modification of the Cys residue at the active site of the EGFR tyrosine kinases. Our previous experience also confirmed the importance of aryl-substituted 4-aminoquinazoline as a key moiety for specific binding at the ATP-binding site of the EGFR tyrosine kinases. Therefore, we hypothesized that proper orientation and distance between the acrylamides and the 4-aminoquinazoline moieties are essential for selective EGFR inhibitors. In particular, we were interested in the introduction of various linkers with limited conformational flexibility. Through extensive research, we identified novel 4-aminoquinazoline with *N*-acryl cyclic unnatural amino acids as potential candidates. Herein, we wish to report our efforts toward the identification of acryloyl-*N*-[4-(arylamino)quinazolin-6-yl]carboxamides as new Her-1/Her-2 dual inhibitors (see Figure 2).

The synthesis of the acryloyl-*N*-[4-(arylamino)quinazolin-6-yl]carboxamide analogs **12** is outlined in Scheme 1. The reaction sequence was initiated using commercially available 2-amino-5-nitrobenzoic acid **6** at an elevated temperature with formamide as a solvent to yield 6-nitroquinazolinone **7**, followed by its chlorination using excessive thionyl chloride and phosphoryl chloride in the presence of a catalytic amount of DMF for preparation of 4-chloroquinazoline **8** with a high yield. The resulting 4-chloroquinazoline **8** was treated with aniline derivatives in refluxing isopropyl alcohol to provide 4-anilino-6-nitroquinazoline **9** with a quantitative yield. After simple filtration of the HCl salts of **9**, key intermediates, *N*-4-aryl-substituted 4-anilino-6-aminoquinazolines **10**, were obtained through reduction of **9** with iron powder in concd HCl. Cyclic amino acid linkers were then introduced at the 6-amino group of **10** through EDCI-mediated amide coupling with various *N*-Boc-protected cyclic amino acids, such as azetidine carboxylic acid, L-proline, and piperidine carboxylic acid. Subsequently, the Boc protecting group was removed by treatment with 30% trifluoroacetic acid in DCM to yield quinazoline derivatives **11**. Finally, EDCI-mediated amide coupling of **11** with acrylic acid provided the desired acryloyl-*N*-[4-(arylamino) quinazolin-6-yl]carboxamide analogs **12** with 14.6% overall yield.

Table 1. In Vitro Cellular Activity[a] of Synthesized Analogs **13**

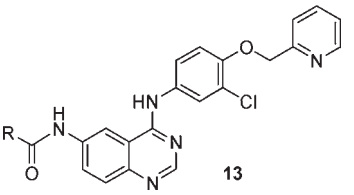

Entry	Compd	R	Cell assay, IC_{50} (nM)	
			A-431[b]	SK-BR3[c]
1	**13a**	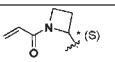	218	13
2	**13b**	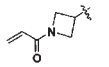	1,400	59
3	**13c**	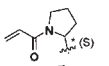	32	10
4	**13d**	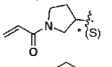	350	49
5	**13e**	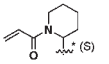	105	14
6	**13f**	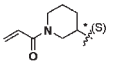	286	39
7	**13g**	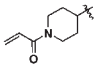	513	71
8	**13h**	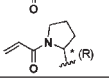	567	2.4
3 (Lapatinib)[d]		-	104	29

[a] All biological data are mean values for three independent experiments performed in duplicate. [b] A431 is Her-1-overexpressing human vaginal epidermoid cancer cell line. [c] SK-Br3 is Her-2-overexpressing human breast cancer cell line. [d] **3** (Lapatinib) was synthesized using the synthetic protocol of WO99/35146.

Biological Effect of the Structures of Carboxamides and Quinazolines Having Various Linker Moieties with Restricted Conformational Flexibility. All synthesized analogs were initially tested for their ability to inhibit cellular proliferation in two representative EGFR-positive cell lines: A431 (Her-1-overexpressing human vaginal epidermoid cancer cell line)[20] and SK-Br3 (Her-2-overexpressing human breast cancer cell line).[21] The orientation of the acrylamide moiety, based on various substituents in the carboxamide moiety of the cyclic amino acids at the C_6 position of the quinazoline core skeleton. As shown in Table 1, the 1-acryloyl-2-carboxamide derivatives of azetidine (**13a**), pyrrolidine (**13c**), and piperidine (**13e**) at the C_6 position of the quinazolines had stronger potency in the A431 cell-based proliferation assay compared to the 1-acryloyl-3-carboxamide derivatives of azetidine (**13b**; entries 1 and 2, IC_{50} = 218 vs 1400 nM), pyrrolidine (**13d**; entries 3 and 4, IC_{50} = 32 vs 350 nM), and piperidine (**13f**; entries 5 and 6, IC_{50} = 105 vs 286 nM). In addition, the

Scheme 2[a]

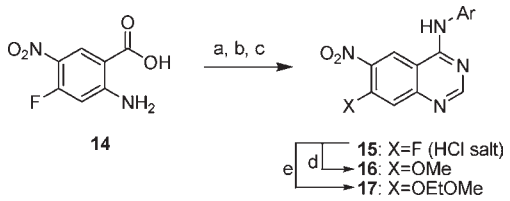

[a] Reagents and conditions: (a) formamide, 170 °C; (b) $SOCl_2$, $POCl_3$, DMF (cat.), reflux; (c) anilines, *i*-PrOH, reflux; (d) sodium methoxide, DMSO, r.t.; (e) 2-methoxyethanol, KOTMS, DMSO, r.t.

1-acryloyl-piperidine-4-carboxamide derivative **13g** (IC_{50} = 513 nM) had diminished potency compared to **13e** and **13f** (entries 5−7). A similar pattern of effects associated with substitution of conformationally rigid linkers at the C_6 position of quinazoline was also observed in the SK-Br3 cell-based proliferation assay; the 1-acryloyl-2-carboxamide derivatives of azetidine (**13a**), pyrrolidine (**13c**), and piperidine (**13e**) at the C_6 position of quinazoline had stronger potency compared to the 1-acryloyl-3-carboxamide derivatives of azetidine (**13b**; entries 1 and 2, IC_{50} = 13 vs 59 nM), pyrrolidine (**13d**; entries 3 and 4, IC_{50} = 10 vs 49 nM), and piperidine (**13f**; entries 5 and 6, IC_{50} = 14 vs 39 nM); furthermore, the 1-acryloyl-piperidine-4-carboxamide **13g** had diminished potency (IC_{50} = 71 nM) compared to **13e** and **13f** (entries 5−7). Potency was also influenced by the stereochemistry of the cyclic amino acids; stronger potency was observed with L-proline (entry 3) than with D-proline (entry 8) as linker moieties with conformational rigidity.

Synthesis and Biological Evaluation of Analogs with C_4- and C_7-Modification of Quinazoline. After optimization of the cyclic linker moiety for proper orientation of the Cys-capturing acrylamide moiety at the C_6 position, we turned our attention to the C_4 and C_7 positions of the quinazoline core skeleton to improve potency. Introduction of substituents such as methoxy and methoxyethyloxy at the C_7 position was pursued with the optimized moiety, *N*-acryloyl-L-proline, at the C_6 position of 6-aminoquinazoline. Systematic replacement of 3-chloro-4-(pyridin-2-ylmethoxy) aniline with various 2, 3, or 4-halogen-substituted anilines was also conducted; notably, 4-fluoro-3-chloroaniline is a moiety shared between **1** (Gefitinib) and **5** (CI-1033). 4-Anilino-7-fluoro-6-nitroquinazolines **15** were prepared according to the modified protocol shown in Scheme 1, beginning with 2-amino-4-fluoro-5-nitrobenzoic acid **14**, followed by treatment with either sodium methoxide or 2-methoxyethanol to yield the C_4- and C_7-modified key intermediates **16** and **17** (see Scheme 2). The final products with C_4- and C_7-modifications (**18** and **19**) were prepared from intermediates **16** and **17** using a process identical to that shown in Scheme 1.

The resulting analogs **18** and **19** were subjected to cellular growth inhibition assays using the Her-1-positive A431 cell line and the Her-2-positive SK-Br3 cell line. As shown in Table 2, replacement of 3-chloro-4-(pyridin-2-ylmethoxy)aniline at the C_4 position of quinazoline (**18a**) with halogen-substituted anilines (**18b**−**d**) in the C_7-methoxy analogs **18** substantially reduced growth inhibition activity against SK-Br3 (IC_{50} = 3 vs 64, 33, and 322 nM, **18a**−**d**, respectively). A similar pattern of reduced activities (1.4- to 2.6-fold, **18c** and **18d** compared to **18a**, respectively) was observed in the Her-1-positive A431 cell proliferation assay, except for the C_4 modification with 4-fluoro-3-chloroaniline derivative **18b**. On the other hand, replacement of 3-chloro-4-(pyridin-2-ylmethoxy) aniline (**19a**)

Table 2. In Vitro Cellular Activity[a] of Synthesized Analogs **18** and **19**

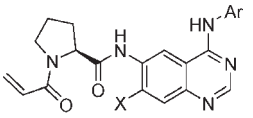

18: X=OCH_3
19: X=$OCH_2CH_2OCH_3$

Compound	Ar	Cell assay, IC_{50} (nM)	
		A-431	SK-Br3
18a	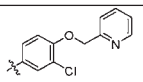	27	3
18b		11	64
18c		70	33
18d		38	222
19a	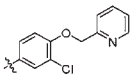	23	3
19b		11	21
19c		8	8
19d		7	7
19e		18	9
19f		6	19
3 (Lapatinib)	-	104	29

[a] All biological data are mean values for three independent experiments performed in duplicate.

with halogen-substituted anilines (**19b**−**f**) at the C_4 position in the C_7-methoxyethyloxy analogs **19** resulted in 1.3- to 3.8-fold enhancement of cellular activities in the A431 assay, but 2.3- to 7-fold reduction of cellular activities in the SK-Br3 assay. Even though the activity reduction in **19c**, **19d**, and **19e** compared to **19a** was observed against SK-Br3 (IC_{50} = 3 vs 8, 7, and 9 nM, 19a, **19c**−**e**, respectively), the selected C_7-methoxyethyloxy analogs (**19c**−**e**) showed high cellular activities in the SK-Br3 assay (IC_{50} < 10 nM).

Based on the results of the cellular growth inhibition assays with the Her-1-positive A431 and the Her-2-positive SK-Br3 cell lines, we selected compounds **19c** and **19d** for further biological evaluation as potential EGFR-targeting therapeutic agents. First, we conducted an enzyme-based inhibition assay with Her-1 and Her-2 tyrosine kinases. In particular, we used a **1** (Gefitinib)- and **2** (Erlotinib)-resistant T790M mutation of Her-1 tyrosine kinase to include drug resistance to these therapeutic agents. As shown in Table 3, **19c** and **19d** demonstrated strong inhibition activities against

Table 3. In Vitro Enzymatic and Cellular Activities[a] of the Synthesized Analogs **19c** and **19d**

	enzyme assay, IC_{50} (nM)			cell assay, IC_{50} (nM)			
compound	Her-1	Her-2	Her-1 T790M	A431	SK-Br3	H1975[b]	Hs27[c]
19c	13	42	24	8	8	213	6603
19d	9	18	11	7	7	63	7442
3 (lapatinib)	52	36	> 1000	104	29	> 1000	> 10000
2 (erlotinib)	> 1000[d]	> 1000	> 1000	96[d]	> 1000	> 1000	> 10000

[a] All biological data are mean values for three independent experiments performed in duplicate. [b] H1975 is an **1** (Gefitinib)/**2** (Erlotinib)-resistant non-small cell lung cancer cell line that harbors the T790 M and L858R mutations. [c] Hs27 is a normal human foreskin cell line. [d] Reported activities in reference, IC_{50} 2 nM against Her-1 [*Cancer Research* **1997**, *57* (21), 4838] and IC_{50} 1.5 μM against A431 [*Proc. Am. Assoc. Cancer Res.* **2005**, *46*, Abstract #1670].

Her-1/Her-2 kinase than **3** (Lapatinib), and **19c** and **19d** also demonstrated excellent potency toward the T790M mutation of Her-1 tyrosine kinase. The additional fluorine at the *para*-position of the C_4-aniline (**19d**) enhanced its potency in the enzymatic inhibition assay as compared to compound **19c**. This conclusion was confirmed by the results of the cell-based proliferation assay. In addition to Her-1-positive A431 and Her-2-positive SK-Br3, we tested **19c** and **19d** with H1975, an **1** (Gefitinib)/**2** (Erlotinib)-resistant non-small cell lung cancer cell line that harbors the T790 M and L858R mutations.[22] This biological evaluation clearly demonstrated that our novel therapeutic agents **19c** and **19d**, have excellent potency as a Her-1/Her-2 dual inhibitor and can overcome clinically frequent drug resistance, having demonstrated strong enzymatic inhibition activity against **1** (Gefitinib)/**2** (Erlotinib)-resistant (T790M) Her-1 tyrosine kinase (**19c**, IC_{50} = 24 nM and **19d**, IC_{50} = 11 nM) and in vitro cellular activity against the **1** (Gefitinib)/**2** (Erlotinib)-resistant cancer cell line H1975 (**19c**, IC_{50} = 213 nM and 19d, IC_{50} = 63 nM). But **19c** and **19d** did not show growth inhibitory activity against normal cell line, Hs27 (**19c**, IC_{50} = 6603 nM and **19d**, IC_{50} = 7442 nM). Next, we checked the selectivity profile of **19c** and **19d** against a panel of 25 kinases including receptor tyrosine kinases, cytoplasmic tyrosine kinases, and serine/threonine kinases. As shown in Table 4, our leading compound **19c** showed excellent activities (IC_{50} < 0.1 μM) against EGFR tyrosine kinases (Her-1, -2, and -4) with superb selectivity. But, we observed some cross-activities (IC_{50} < 0.1 μM) in the case of **19d** against Ret, Lck, Abl1, and Src. Lastly, we tested the mode of action of **19c** using an A431 cell washout experiment. The phosphorylation rate of EGFR after medium washout was measured using Western blot analysis. After 8 h of medium washout, only 15% of EGFR was phosphorylated when A431 cells were treated with **19c**. In comparison, **2** (Erlotinib)-treated cells restored their 100% phosphorylation on EGFR in 8 h after medium washout. The significant reduction in the phosphorylation rate of EGFR suggests that our novel therapeutic agent **19c** has an irreversible binding mode of action toward EGFR.[25]

Pharmacokinetic Studies and In Vivo Efficacy of 19c and 19d. Prior to clinical studies, our leading novel compounds **19c** and **19d** were subjected to pharmacokinetic studies in male rats. For an in vivo study, **19c** and **19d** were prepared as hydrochloride salt and mesylate, respectively. As shown in Table 5, pharmacokinetic parameters for **19c** and **19d** were determined after a single oral administration (10 mg/kg) and intravenous injection (5 mg/kg). The selected compounds demonstrated fair oral bioavailability (**19c**, 76.5% and **19d**, 24.8%) and desirable exposure levels (C_{max} and AUC) in the rats. To evaluate their anticancer efficacy in vivo, **19c** and **19d** were dosed in female nude mice xenografted with Her-1-positive A431 cell lines. The in vivo efficacies of compounds **19c** and **19d** were compared to **3** (Lapatinib) as a positive control; the dose of each agent (3 mg/kg for **19c**−**d** and 10 mg/kg for **3**) was selected based on their in vitro enzymatic and cellular activities such that a comparable efficacy was obtained in all treatment groups. After once-daily oral dosing for 11 days, compounds **19c** and **19d** produced a significant reduction in tumor size (inhibition rate[23] on day 11: 66% for **19c**, 74% for **19d**). In comparison, **3** (Lapatinib) had a marginal effect on tumor reduction (4.5%) even at a 10 mg/kg dosage. Change in body weight was also monitored

Table 4. Selectivity Profile of Synthesized Analogs **19c** and **19d** against 25 Kinases[a]

IC_{50}[b] (μM)	**19c**	**19d**
Receptor Tyrosine Kinase		
Her-1	< 0.1	< 0.1
Her-2	< 0.1	< 0.1
Her-4	< 0.1	< 0.1
Flt-1	> 10.0	10.0
KDR	1.3	0.6
Flt-4	2.7	4.5
Flt-3	> 10.0	> 10.0
PDGFRα	> 10.0	> 10.0
PDGFRβ	> 10.0	> 10.0
IGF-1R	> 10.0	> 10.0
Kit	> 10.0	> 10.0
FGFR1	> 10.0	> 10.0
FGFR2	4.1	2.0
Ret	0.7	< 0.1
Tek	5.0	2.2
Met	> 10.0	> 10.0
Cytoplasmic Tyrosine Kinase		
Lck	0.3	< 0.1
Abl1	0.5	< 0.1
Src	0.8	< 0.1
Serine/Threonine Kinase		
Akt1	> 10.0	> 10.0
AuroraB	> 10.0	> 10.0
CDK2	> 10.0	> 10.0
MAPK1	> 10.0	> 10.0
Raf1	10.0	10.0
PKCα	> 10.0	> 10.0

[a] This test was conducted by Invitrogen Select Screen Biochemical Kinase (SSBK) Profiling Service. [b] The IC_{50} was calculated from data at three different concentrations: 0.1, 1, and 10 μM.

Table 5. Pharmacokinetic Profiles of Selected Compounds in Male Rats

parameters (po)	**19c**[a,c]	**19d**[b,c]
AUC_{last} (ng·h/mL)	2019.3 ± 205.2	428.50 ± 27.91
C_{max} (ng/mL)	1745.7 ± 170.2	146.86 ± 17.42
$T_{1/2}$ (h)	3.2 ± 0.7	4.2 ± 1.1
F (%)	76.5	24.8

[a] **19c** was treated as HCl salt. [b] **19d** was treated as mesylate. [c] The used vehicle was 20% PEG400 in distilled water and the pharmacokinetic parameters were determined after a single oral administration (10 mg/kg, n = 5) and intravenous injection (5 mg/kg, n = 3).

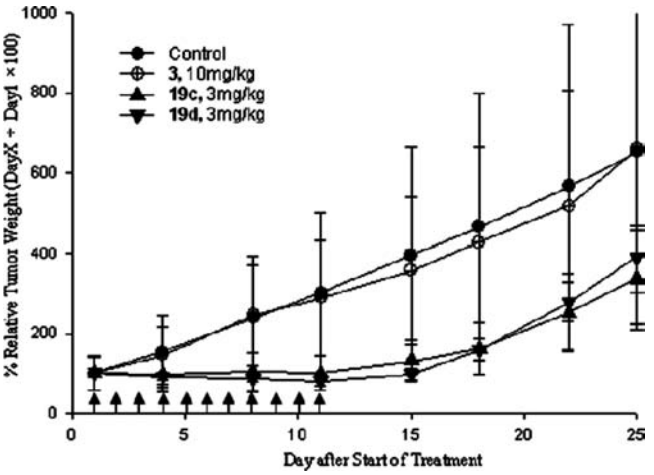

Figure 3. Antitumor activity during treatment with **19c** (as HCl salt), **19d** (as mesylate), **3** (Lapatinib), or vehicle control in an A431-xenograft model in nude mice. Each compound was administered through once-daily oral treatments for 11 days from the 7th day after implantation. The used vehicle was 20% PEG400 in distilled water. Compounds **19c** (as HCl salt), **19d** (as mesylate), and **3** (Lapatinib) were administered at 3, 3, and 10 mg/kg, respectively. Initial group size was eight animals for all groups. All biological data were obtained from a single experiment.

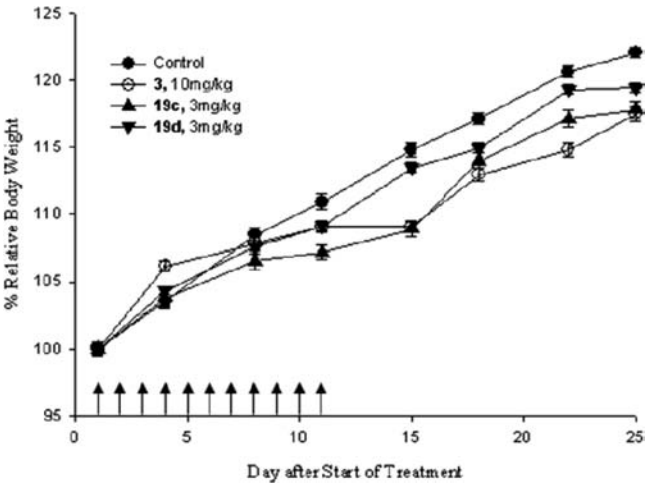

Figure 4. Body weight change during treatment with **19c** (as HCl salt), **19d** (as mesylate), **3** (Lapatinib), or the vehicle control in an A431-xenograft model in nude mice. See Figure 3 for detailed study conditions.

during the in vivo efficacy experiment. As shown in Figure 4, significant body-weight loss was not observed during treatment with **19c** and **19d**, consistent with treatment with **3** (Lapatinib) or no treatment. To examine the tolerability of our leading agent **19c**, we conducted secondary in vivo experiment with oral administration of **19c** at raised doses for 11 days in A431-xenografted nude mice. Even at high doses of **19c** (12.5, 25, and 50 mg/kg), the body-weight change was within 5% (compared to their initial body-weight), which confirms that our novel therapeutic agent **19c** has high safety margin in in vivo systems (see Figure 5).

Summary

Herein, we have described the synthesis of a novel series of (*S*)-1-acryloyl-*N*-[4-(arylamino)-7-(alkoxy)quinazolin-6-yl]-pyrrolidine-2-carboxamides, which are potent Her-1/Her-2

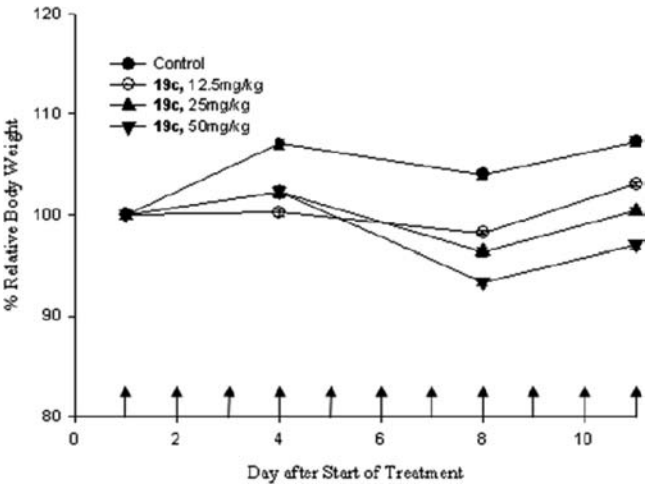

Figure 5. Body weight change during treatment with **19c** (as HCl salt) at higher doses (12.5, 25, and 50 mg/kg) or the vehicle control in an A431-xenograft model in nude mice. See Figure 3 for details of study conditions.

dual inhibitors for the treatment of **1** (Gefitinib)/**2** (Erlotinib)-resistant non-small cell lung cancer. In contrast to the Her-1 selective inhibitors, **1** and **2**, our novel compounds are irreversible inhibitors of Her-1 and Her-2 tyrosine kinases with the potential to overcome clinically relevant, mutation-induced drug (**1** and **2**) resistance.[24] SAR studies of these series identified that the preferred orientation and special location of Cys-capturing acrylamide moiety from the key binding motif, 6-aminoquinazoline. Based on our systematic structural modification on the linker region, conformationally rigid L-proline at the C_6 position showed the strongest potency for Her-1/Her-2 dual inhibition activity. In addition, methoxyethyloxy functionality at the C_7 position of the quinazoline and di- or trihalogen-substituted anilines at the C_4 position were essential for enhanced efficacy in in vitro enzymatic as well as in vitro cellular assays. The selected compounds (**19c** and **19d**) showed excellent EGFR inhibition activity even toward the **1** (Gefitinib)- and **2** (Erlotinib)-resistant T790M mutation of Her-1 tyrosine kinase. The leading compound **19c** also showed excellent selectivity in an enzyme-based inhibition assay with a panel of 25 kinases. We confirmed that our leading Her-1/Her-2 dual inhibitor (**19c**) has an irreversible binding mode[25] to EGFR through a cell washout test, without cellular toxicity toward a normal cell line (Hs27). The excellent pharmacokinetic profiles of these compounds in rats and their robust in vivo efficacy in an A431-xenograft model clearly demonstrated that they merit further investigation as novel therapeutic agents for EGFR-targeting treatment of solid tumors, especially **1** (Gefitinib)/**2** (Erlotinib)-resistant non-small cell lung cancer.

Experimental Section

Chemistry. General Information. All commercial chemicals and solvents were reagent grade and were used without further purification unless otherwise specified. All reported yields are isolated yields after chromatography or crystallization. ^{1}H and ^{13}C NMR spectra were recorded on a Bruker DRX-300 (Bruker Biospin, Germany) and Varian Inova-500 (Varian Assoc., Palo Alto, CA), Chemical shifts are reported in ppm relative to the residual solvent peak ($CDCl_3$, ^{13}C 77.00; TMS: 0.00). Multiplicity was indicated as follows: s (singlet); d (doublet); t (triplet); q (quartet); m (multiplet); dd (doublet of doublet); ddd (doublet

of doublet of doublet); dt (triplet of doublet); td (doublet of triplet); br s (broad singlet), and so on. The high resolution mass spectrometric analyses were conducted at the Mass Spectrometry Laboratory of Seoul National University using mass spectrometer by direct injection for fast atomic bombardment (FAB). Products were purified by flash column chromatography on silica gel (230−400 mesh). The eluent used for purification is reported in parentheses. High performance liquid chromatography analyses for checking purity (>95% area) of synthesized compounds were performed on SHIMADZU HPLC equipped with a reverse phase column (XDB C18, 5 μm, 4.6 × 150 mm). Samples were analyzed starting with 5% ACN in H_2O (0.1% TFA) for 5 min after injected 10 μL of sample and solvent was changed from 5% ACN in H_2O (0.1% TFA) to 100% ACN (0.1% TFA) for 45 min with 1.0 mL/min flow. Absorbance was detected by 254 nm. Thin-layer chromatography (TLC) was performed on precoated glass-backed plates (silica gel 60 F_{254} 0.25 mm), and the components were visualized by observation under UV light (254 and 365 nm) or by treating the plates with anisaldehyde, $KMnO_4$, and phosphomolybdic acid followed by heating. Distilled water was polished using ion exchange and filtration.

General Procedures for the Synthesis of 13a−h. To a stirred solution of N^4-[3-chloro-4-(pyridin-2-ylmethoxy)phenyl]quinazoline-4,6-diamine[24] (150 mg, 0.4 mmol) in pyridine (6 mL) were added the appropriate *N*-Boc-amino acid (1.0 mmol) and 1-(3-dimethylaminopropy1)-3-ethylcarbodiimide hydrochloride (300 mg, 1.5 mmol). After being stirred at room temperature for 2 h, the reaction mixture was distilled under reduced pressure to remove pyridine and diluted with water, the aqueous layer was extracted three times with a mixture of chloroform and isopropanol (3:1), and the organic extract was washed with water and brine and dried over anhydrous sodium sulfate. The solvent was evaporated and the crude mixture was dried under reduced vacuum. The resulting residue was dissolved in a mixture of methylene chloride (7 mL) and trifluoroacetic acid (3 mL) and stirred at room temperature for 1 h. The resulting reaction mixture was concentrated under reduced pressure and saturated sodium bicarbonate (aq) was added slowly to the resulting residue while stirring to make it weakly alkaline. The reaction mixture thus obtained was extracted with a mixture of chloroform and isopropanol (3:1). The combined organic extract was dried over anhydrous sodium sulfate and concentrated under a reduced pressure to obtain a crude product, which was purified by silica gel flash column chromatography (methanol/chloroform = 1:9). To a stirred solution of acrylic acid (15 μL, 0.22 mmol) in THF (2 mL) at 0 °C were added 1-(3-dimethylaminopropy1)-3-ethylcarbodiimide hydrochloride (48 mg, 0.25 mmol), pyridine (20 μL, 0.25 mmol), and the purified compound (100 mg, 0.21 mmol). After being stirred at 0 °C for 1 h, the reaction mixture was diluted with sodium bicarbonate aqueous solution, the aqueous layer was extracted three times with chloroform, and the organic extract was washed with water and brine and dried over anhydrous sodium sulfate. The solvent was evaporated and the crude mixture was purified by silica gel flash column chromatography (methanol/ethyl acetate/methylene chloride = 1:7:7) to obtain a desired product.

(*S*)-1-Acryloyl-*N*-[4-(3-chloro-4-(pyridin-2-ylmethoxy)phenylamino)quinazolin-6-yl]azetidine-2-carboxamide (13a). Pale yellow solid, 89% yield. ^{1}H NMR ($CDC1_3$, 300 MHz): δ 9.95 (s, 1H), 8.82 (d, 1H), 8.69 (s, 1H), 8.59 (d, 1H), 7.91(d, 1H), 7.88 (d, 1H), 7.73 (td, 1H), 7.66 (m, 1H), 7.54 (td, 2H), 7.24 (m, 1H), 7.02 (d, 1H), 5.30 (s, 2H), 4.51 (t, 1H), 3.90 (q, 1H), 3.42 (m, 1H), 2.77 (m, 1H), 2.50 (m, 1H).

1-Acryloyl-*N*-[4-(3-chloro-4-(pyridin-2-ylmethoxy)phenylamino)-quinazolin-6-yl]azetidine-3-carboxamide (13b). Pale yellow solid, 55% yield. ^{1}H NMR ($CDC1_3$, 300 MHz): δ 8.85 (s, 1H), 8.79 (s, 1H), 8.70 (s, 1H), 8.60 (d, 1H), 7.89 (d, 1H), 7.86 (d, 1H), 7.76 (t, 1H), 7.66 (d, 1H), 7.51 (m, 2H), 7.03 (d, 1H), 5.31 (s, 2H), 4.01 (t, 2H), 3.85 (t, 2H), 3.40 (m, 1H).

(*S*)-1-Acryloyl-*N*-[4-(3-chloro-4-(pyridin-2-ylmethoxy)phenylamino)quinazolin-6-yl]pyrrolidine-2-carboxamide (13c). Pale yellow solid, 57% yield. ^{1}H NMR (DMSO-d_6, 300 MHz): δ 10.22 (s, 1H), 9.65 (s, 1H), 8.54 (d, 1H), 8.45 (s, 1H), 8.17 (d, 1H), 7.95 (s, 1H), 7.82 (t, 1H), 7.67 (m, 2H), 7.52 (d, 1H), 7.30 (t, 1H), 7.20 (d, 1H), 5.23 (s, 2H), 3.75 (m, 1H), 2.88 (m, 2H), 2.01 (m, 1H), 1.80 (m, 1H), 1.64 (m, 2H).

(*S*)-1-Acryloyl-*N*-[4-(3-chloro-4-(pyridin-2-ylmethoxy)phenylamino)quinazolin-6-yl]pyrrolidine-3-carboxamide (13d). Pale yellow solid, 55% yield. ^{1}H NMR ($CDCl_3$, 300 MHz): δ 8.59 (m, 3H), 7.76−7.61 (m, 5H), 7.45 (d, 1H), 7.23 (t, 1H), 6.93 (d, 1H), 6.32 (m, 2H), 5.68 (m, 1H), 5.24 (s, 2H), 4.88 (bs, 1H), 3.80 (m, 2H), 3.58 (m, 1H), 3.15 (m, 1H), 2.40 (m, 1H), 2.20 (m, 1H).

(*S*)-1-Acryloyl-*N*-[4-(3-chloro-4-(pyridin-2-ylmethoxy)phenylamino)quinazolin-6-yl]piperidine-2-carboxamide (13e). Pale yellow solid, 57% yield. ^{1}H NMR ($CDCl_3$, 300 MHz): δ 9.27 (s, 1H), 8.65 (s, 1H), 8.60 (d, 1H), 8.45 (s, 1H), 7.90 (d, 1H), 7.76 (t, 2H), 7.67 (d, 1H), 7.54 (m, 3H), 7.30 (d, 1H), 6.65 (dd, 1H), 6.44 (dd, 1H), 5.85 (dd, 1H), 4.00 (d, 1H), 3.25 (t, 1H), 2.30 (d, 1H), 2.03−1.58 (m, 6H).

(*S*)-1-Acryloyl-*N*-[4-(3-chloro-4-(pyridin-2-ylmethoxy)phenylamino)quinazolin-6-yl]piperidine-3-carboxamide (13f). Pale yellow solid, 43% yield. ^{1}H NMR ($CDCl_3$, 300 MHz): δ 9.63 (s, 1H), 8.76 (s, 1H), 8.68 (s, 1H), 8.60 (d, 1H), 7.84 (m, 2H), 7.76 (m, 2H), 7.66 (d, 1H), 7.55 (m, 2H), 7.02 (d, 1H), 6.59 (dd, 1H), 6.39 (d, 1H), 5.81 (d, 1H), 5.30 (s, 2H), 4.43 (d, 1H), 3.77 (m, 1H), 3.64 (m, 1H), 3.49 (m, 1H), 2.80 (m, 1H), 2.48 (m, 1H), 1.70 (m, 3H).

1-Acryloyl-*N*-[4-(3-chloro-4-(pyridin-2-ylmethoxy)phenylamino)-quinazolin-6-yl]piperidine-4-carboxamide (13g). Pale yellow solid, 11% yield. ^{1}H NMR ($CDCl_3$, 300 MHz): δ 8.76 (s, 1H), 8.69 (s, 1H), 8.60 (d, 1H), 7.85 (m, 2H), 7.75 (m, 1H), 7.66 (m, 1H), 7.50 (m, 2H), 7.42 (d, 1H), 7.01 (d, 1H), 6.58 (dd, 1H), 6.30 (dd, 1H), 5.73 (dd, 1H), 5.29 (s, 2H), 4.70 (bs, 1H), 3.20 (m, 1H), 2.80 (m, 2H), 2.50 (m, 1H), 1.82 (m, 4H).

(*R*)-1-Acryloyl-*N*-[4-(3-chloro-4-(pyridin-2-ylmethoxy)phenylamino)quinazolin-6-yl]pyrrolidine-2-carboxamide (13h). Pale yellow solid, 68% yield. ^{1}H NMR (DMSO-d_6, 300 MHz): δ 10.22 (s, 1H), 9.65 (s, 1H), 8.54 (d, 1H), 8.45 (s, 1H), 8.17 (d, 1H), 7.95 (s, 1H), 7.82 (t, 1H), 7.67 (m, 2H), 7.52 (d, 1H), 7.30 (t, 1H), 7.20 (d, 1H), 5.23 (s, 2H), 3.75 (m, 1H), 2.88 (m, 2H), 2.01 (m, 1H), 1.80 (m, 1H), 1.64 (m, 2H).

General Procedures for the Synthesis of 18a−d and 19a−f. The synthesis of **18a−d** and **19a−f** was performed using similar protocols for the synthesis of **13a−h** except using appropriate anilines[24] and *N*-(*t*-butoxycarbonyl)-L-proline instead of N^4-(3-chloro-4-(pyridin-2-ylmethoxy)phenyl)quinazoline-4,6-diamine[24] and the appropriate *N*-Boc-amino acid.

(*S*)-1-Acryloyl-*N*-[4-(3-chloro-4-(pyridin-2-ylmethoxy)phenylamino)-7-methoxyquinazolin-6-yl]pyrrolidine-2-carboxamide (18a). Pale yellow solid, 25% yield. ^{1}H NMR (CD_3OD, 300 MHz): δ 8.76 (s, 1H), 8.55 (d, 1H), 8.40 (s, 1H), 7.88 (m, 2H), 7.71 (d, 1H), 7.55 (dd, 1H), 7.33 (t, 1H), 7.12 (m, 2H), 6.71 (dd, 1H), 6.36 (d, 1H), 5.82 (d, 1H), 5.23 (s, 2H), 4.85 (m, 1H), 4.02 (s, 3H), 3.81 (m, 2H), 2.03−2.27 (m, 4H).

(*S*)-1-Acryloyl-*N*-[4-(3-chloro-4-fluorophenylamino)-7-methoxyquinazolin-6-yl]pyrrolidine-2-carboxamide (18b). White solid, 42% yield. ^{1}H NMR (DMSO-d_6, 300 MHz): δ 9.65 (s, 1H), 8.76 (s, 1H), 8.57 (s, 1H), 8.28 (s, 1H), 7.85 (dd, 1H), 7.57 (m, 1H), 7.08 (t, 1H), 6.98 (s, 1H), 6.55 (dd, 1H), 6.42 (dd, 1H), 5.78 (dd, 1 H), 4.95 (d, 1H), 3.76 (s, 3H), 3.76 (m, 1H), 3.65 (m, 1H), 2.50 (m, 1H), 2.10 (m, 3H).

(*S*)-1-Acryloyl-*N*-[4-(3-chloro-2-fluorophenylamino)-7-methoxyquinazolin-6-yl]pyrrolidine-2-carboxamide (18c). White solid, 28% yield. ^{1}H NMR (DMSO-d_6, 300 MHz): δ 9.83 (s, 1H), 9.52 (s, 1H), 8.81 (s, 1H), 8.06 (m, 1H), 7.73 (m, 1H), 7.38 (m, 1H), 7.27 (s, 1H), 6.67 (m, 1H), 6.20 (m, 1H), 5.74 (m, 1H), 4.73 (m, 1H), 4.30 (m, 2H), 3.63 (m, 2H), 3.61 (m, 2H), 3.32 (s, 3H), 2.09 (m, 2H), 1.95 (m, 2H).

(*S*)-1-Acryloyl-*N*-[4-(3-chloro-4-(pyridin-2-ylmethoxy)phenylamino)-7-(2-methoxyethoxy) quinazolin-6-yl]pyrrolidine-2-carboxamide (19a). Pale yellow solid, 60% yield. ^{1}H NMR (DMSO-d_6, 300 MHz): δ 10.61 (s, 1H), 9.71 (s, 1H), 9.05 (s, 1H), 8.59 (d, 1H), 8.45 (s, 1H), 8.31 (s, 1H), 7.93 (d, 1H), 7.88 (td, 1H), 7.64 (dd, 1H), 7.58 (d, 1H), 7.37 (m, 2H), 7.28 (s, 2H), 7.23 (d, 1H), 5.28 (s, 2H), 4.36 (t, 2H), 3.82 (m, 1H), 3.79 (t, 2H), 3.40 (s, 3H), 2.68 (m, 2H), 2.10 (m, 2H), 1.67 (m, 2H).

(*S*)-1-Acryloyl-*N*-[4-(3-chloro-4-fluorophenylamino)-7-(2-methoxyethoxy)quinazolin-6-yl]pyrrolidine-2-carboxamide (19b). White solid, 28% yield. ^{1}H NMR (DMSO-d_6, 300 MHz): δ 9.83 (s, 1H), 9.52 (s, 1H), 8.81 (s, 1H), 8.06 (m, 1H), 7.73 (m, 1H), 7.38 (m, 1H), 7.27 (s, 1H), 6.67 (m, 1H), 6.20 (m, 1H), 5.74 (m, 1H), 4.73 (m, 1H), 4.30 (m, 2H), 3.63 (m, 2H), 3.61 (m, 2H), 3.32 (s, 3H), 2.09 (m, 2H), 1.95 (m, 2H).

(*S*)-1-Acryloyl-*N*-[4-(3-chloro-2-fluorophenylamino)-7-(2-methoxyethoxy)quinazolin-6-yl]pyrrolidine-2-carboxamide (19c). White solid, 10% yield. ^{1}H NMR ($CDCl_3$, 300 MHz): δ 9.99 (s, 1H), 9.07 (s, 1H), 8.68 (s, 1H), 8.39 (dd, 1H), 7.53 (s, 1H), 7.14 (d, 2H), 6.55 (d, 1H), 6.53 (s, 1H), 5.82 (dd, 1H), 4.94 (d, 1H), 4.34 (m, 2H), 3.96 (m, 2H), 3.77 (td, 1H), 3.62 (m, 1H), 3.50 (s, 3H), 2.64 (m, 1H), 2.14 (m, 2H), 1.95 (m, 1H); ^{13}C NMR (125 MHz, $CDCl_3$): δ 169.8, 166.1, 156.4, 154.0, 152.7, 148.3, 129.2, 129.1, 127.9, 124.8, 124.4, 122.3, 121.8, 121.0, 109.6, 109.0, 107.5, 70.4, 68.4, 60.9, 59.1, 47.5, 26.9, 25.1; HRMS (FAB$^+$) m/z calcd for $C_{25}H_{25}ClFN_5O_4$ [M + H]$^+$: 514.1657. Found: 514.1658.

(*S*)-1-Acryloyl-*N*-[4-(3-chloro-2,4-difluorophenylamino)-7-(2-methoxyethoxy)quinazolin-6-yl]pyrrolidine-2-carboxamide (19d). White solid, 14% yield. ^{1}H NMR ($CDC1_3$, 300 MHz): δ 9.95 (s, 1H), 9.03 (s, 1H), 8.60 (s, 1H), 8.06 (m, 1H), 7.62 (bs, 1H), 7.21 (s, 1H), 7.01 (m, 1H), 6.53 (m, 2H), 5.82 (m, 1H), 4.94 (m, 1H), 4.30 (m, 2H), 3.94 (m, 2H), 3.76 (m, 1H), 3.62 (m, 1H), 3.49 (s, 3H), 2.58 (m, 1H), 2.33 (m, 1H), 2.13 (m, 2H), 1.95 (m, 1H); ^{13}C NMR (125 MHz, $CDCl_3$ + CD_3OD, 1 drop): δ 170.1, 170.0, 166.0, 157.3, 154.2, 152.7, 152.6, 148.1, 129.3, 128.3, 127.8, 123.8, 123.7, 111.2, 111.1, 110.0, 109.3, 107.1, 70.3, 68.2, 60.9, 59.0, 47.5, 27.4, 25.0; HRMS (FAB$^+$) m/z calcd for $C_{25}H_{24}ClF_2N_5O_4$ [M + H]$^+$: 532.1563. Found: 532.1575.

(*S*)-1-Acryloyl-*N*-[4-(3,4-dichloro-2-fluorophenylamino)-7-(2-methoxyethoxy)quinazolin-6-yl]pyrrolidine-2-carboxamide (19e). White solid, 10% yield. ^{1}H NMR ($CDC1_3$, 300 MHz): δ 10.03 (s, 1H), 9.06 (s, 1H), 8.67 (s, 1H), 8.36 (t, 1H), 7.52 (s, 1H), 7.30 (dd, 1H), 7.24 (s, 1H), 6.55 (m, 2H), 5.83 (m, 1H), 4.95 (m, 1H), 4.33 (m, 2H), 3.95 (m, 2H), 3.76 (m, 1H), 3.62 (m, 1H), 3.51 (s, 3H), 2.61 (m, 1H), 2.13 (m, 2H), 1.97 (m, 1H).

(*S*)-1-Acryloyl-*N*-[4-(4-bromo-3-chloro-2-fluorophenylamino)-7-(2-methoxyethoxy)quinazolin-6-yl]pyrrolidine-2-carboxamide (19f). Ivory solid, 31% yield. ^{1}H NMR ($CDCl_3$, 300 MHz): δ 9.99 (s, 1H), 9.05 (s, 1H), 8.65 (s, 1H), 8.20 (t, 1H), 7.70 (bs, 1H), 7.43 (dd, 1H), 7.25 (s, 1H), 6.55 (m, 2H), 5.83 (m, 1H), 4.94 (m, 1H), 4.32 (m, 2H), 3.94 (m, 2H), 3.78 (m, 1H), 3.60 (m, 1H), 3.5 (s, 3H), 2.61 (m,1H), 2.10 (m, 3H).

(*S*)-1-Acryloyl-*N*-[4-(3-chloro-2-fluorophenylamino)-7-(2-methoxyethoxy)quinazolin-6-yl]pyrrolidine-2-carboxamide Hydrochloride (19c HCl). To a stirred solution of **19c** (1.0 g, 1.95 mmol) in isopropanol (20 mL) was slowly added 1 N HCl ethereal solution (4.88 mL, 4.88 mmol). After being stirred at room temperature for 1 h, the regenerated solid was collected through simple filtration with quick wash by cooled isopropanol and dried under reduced pressure. White solid, 94% yield. ^{1}H NMR ($CDCl_3$, 300 MHz): δ 10.38 (s, 1H), 9.22 (s, 1H), 8.80 (s, 1H), 8.66 (s, 1H), 8.04 (s, 1H), 7.90 (t, 1H), 7.39 (t, 1H), 7.25 (td, 1H), 6.54 (d, 2H), 5.85 (t, 1H), 4.95 (d, 1H), 4.45 (m, 2H), 3.95 (m, 2H), 3.70 (m, 1H), 3.50 (m, 1H), 3.48 (s, 3H), 2.50 (m, 1H), 2.14 (m, 2H), 2.00 (m, 1H); ^{13}C NMR (125 MHz, $CDCl_3$): δ 170.4, 166.0, 159.3, 155.0, 153.5, 151.5, 148.4, 136.8, 130.3, 129.5, 129.3, 127.9, 126.0, 124.6, 121.9, 111.6, 106.9, 100.2, 70.0, 69.6, 61.0, 59.1, 47.9, 27.4, 25.2.

(*S*)-1-Acryloyl-*N*-[4-(3-chloro-2,4-difluorophenylamino)-7-(2-methoxyethoxy)quinazolin-6-yl]pyrrolidine-2-carboxamide Mesylate (19d Mesylate). To a stirred solution of **19d** (1.0 g, 1.88 mmol) in ethyl acetate (20 mL) was slowly added methanesulfonic acid (0.27 mL, 4.14 mmol). After being stirred at room temperature for 2 h, the regenerated solid was collected through simple filtration with quick wash by cooled ethyl acetate and dried under reduced pressure. Ivory solid, 86% yield. ^{1}H NMR ($CDCl_3$, 500 MHz): δ 9.85 (s, 1H), 9.09 (s, 1H), 8.53 (s, 1H), 7.61 (m, 1H), 7.56 (s, 1H), 7.07 (m, 1H), 6.53 (dd, 1H), 6.44 (d, 1H), 5.85 (dd, 1H), 4.89 (t, 1H), 4.34 (m, 1H), 4.23 (m, 1H), 3.90 (m, 1H), 3.79 (m, 2H), 3.65 (m, 1H), 3.42 (s, 3H), 2.91 (s, 6H), 2.41 (m, 1H), 2.11 (m, 3H); ^{13}C NMR (125 MHz, $CDCl_3$): δ 170.2, 166.4, 159.5, 155.7, 154.6, 148.8, 136.8, 130.4, 130.1, 127.4, 125.8, 112.6, 111.8, 111.7, 110.9, 106.7, 100.3, 70.0, 69.8, 61.2, 58.9, 47.9, 39.3, 27.8, 24.9.

General Procedures for the EGFR Enzyme Assay. A total of 10 μL of EGFR enzyme (Her-1, Her-2, or Her-1 T790 M kinase, Upstate) was added to each well of a 96-well microplate. As an EGFR inhibitor, 10 μL of serially diluted solution of the synthesized compounds was added to the individual wells, and the plate was incubated at room temperature for 10 min. A total of 10 μL of Poly (Glu, Tyr 4:1, Sigma) and 10 μL of ATP were successively added to initiate a kinase reaction, and the resulting mixture was incubated at room temperature for 1 h. A total of 10 μL of 100 mM EDTA was added to each well and stirred for 5 min to terminate the kinase reaction. Then 10 μL of 10× antiphosphotyrosine antibody (Pan Vera), 10 μL of 10× protein tyrosine kinase (PTK) green tracer (Pan Vera), and 30 μL of fluorescence polarization (FP)-diluted buffer were added to the reacted mixture, followed by incubation in the dark at room temperature for 30 min. The FP value of each well was determined using a VICTORIII fluorescence meter (Perkin-Elmer) at 488 nm. The IC_{50}, that is, the concentration at which 50% inhibition was observed, was determined by setting the maximum value (0% inhibition) to the polarized light value for a well untreated with EGFR inhibitor and the minimum value (100% inhibition). IC_{50} calculations and analysis were carried out using Microsoft Excel.

General Procedures for the Cell Growth Inhibitory Assay. A human vaginal epidermoid cancer cell line, A431 (ATCC: CRL-1555), a human breast cancer cell line, SK-Br3 (ATCC: HTB-30), and a primary human fibroblast cell-line, Hs27 (ATCC: CCL-34), were used to measure the inhibitory activities of the synthesized compounds toward cancer cell growth and cytotoxicity to normal cells. Cells were cultured in Dulbecco's modified Eagle's medium (DMEM) with 4.5 g/L glucose and 1.5 g/L sodium bicarbonate, and were supplemented with 10% fetal bovine serum (FBS). In addition, an Gefitinib/Erlotinib-resistant non-small cell lung cancer cell line, H1975 (ATCC: CRL-5908), was incubated in an RPMI medium containing 1% sodium pyruvate and 10% FBS. These cell lines, stored in a liquid nitrogen tank, were quickly thawed at 37 °C and centrifuged to remove the medium. The resulting cell pellet was mixed with the culture medium and incubated in a culture flask at 37 °C under 5% CO_2 for 2−3 days; thereafter, the medium was removed. The remaining cells were washed with Dulbecco's phosphate buffered saline (DPBS) and were separated from the flask using Trypsin-EDTA. The separated cells were diluted with the culture medium to a concentration of 100000 cells/mL for A431 or Hs27 or 200000 cells/mL for SK-Br3. A total of 100 μL of the diluted cell solution was added to each well of a 96-well plate and incubated at 37 °C under 5% CO_2 for 1 day.

The synthesized compounds were dissolved in 99.5% DMSO to a concentration of 25 mM. If the test compound was not soluble in DMSO, a small amount of 1% HCl was added and the mixture was held in a 40 °C water bath for 30 min until complete dissolution was achieved. The test compound solution was diluted with culture medium to a final concentration of 100 μM and then diluted 10 times serially to 10^{-6} μM (the final concentration of DMSO was less than 1%). The medium was then removed from each of 96 wells of the microplate. A total of 100 μL of the test compound solution was added to each well

holding the cultured cells, and the microplate was incubated at 37 °C under 5% CO_2 for 72 h. After removing the medium from the plate, 50 μL 10% trichloroacetic acid was added to each well, and the plate was maintained at 37 °C for 1 h to fix the cells to the bottom of the plate. Trichloroacetic acid was removed from each well, the plate was dried, 100 μL of SRB dye solution was added, and the resulting mixture was reacted for 10 min. The SRB dye solution was prepared by dissolving SRB in 1% acetic acid to a concentration of 0.4% by wt. After removing the dye solution, the plate was washed with water and dried. If the dye solution was not effectively removed by washing with water, 1% acetic acid was used. Trizma base (10 mM) in the amount of 150 μL was added to each well, and absorbance at 570 nm was determined using a microplate reader. For H1975, the cells were diluted with the culture medium to a concentration of 50000 cells/mL. Diluted cell solution (100 μL) was added to each well of a 96-well microplate, and after 1 day of incubation at 37 °C under 5% CO_2, each well was washed with a mixture of RPMI, 0.1% FBS, and 1% penicillin-streptomycin (PS), followed by replacement of the medium. The plate was held overnight and treated with various concentrations under the same medium conditions for 48 h. Similar to an MTT assay, 15 μL of a CellTiter oneshot solution (Promega) was added to each well and incubated for 2−3 h, and the absorbance at 490 nm was determined. The IC_{50} value was calculated based on the difference between the final concentration of test cells and the initial concentration of the cells incubated in a well untreated with the test compound which was considered 100%. IC_{50} calculations were carried out using Microsoft Excel.

Pharmacokinetic Studies. Male rats (Sprague−Dawley rats, body-weight range: 250 ± 10 g, i.v.: n = 3, p.o.: n = 5) were administered the test compounds intravenously via the tail vein at 5 mg/kg or orally at 10 mg/kg by gavage in a solution of 20% PEG400 in distilled water. For the in vivo study, **19c** and **19d** were prepared as HCl salt and mesylate, respectively. At predetermined times 24 h or more after dosing, 0.3 mL of blood was collected from the jugular vein using a tube containing anticoagulant (1000 IU/mL, heparin, 3 μL). The plasma was separated by centrifugation (12000 rpm, 2 min, Eppendorf). The concentrations of the compounds were measured in the plasma using LC/MS/MS after protein precipitation with acetonitrile. The relevant estimated pharmacokinetic parameters for plasma were derived using WinNonlin Version 5.2 (Pharsight).

In Vivo Efficacy Study. A total of 30 mg of mouse A431 tumor fragments was implanted subcutaneously into the right flank of NU/NU Balb/C mice (female, body-weight range: 20 ± 5 g). Treatment was initiated approximately 7 days after implantation. Animals were randomized into treatment groups (n = 8) with similar mean tumor volumes in milligrams[26] of 187.4 mg. For the in vivo study, **19c** and **19d** were prepared as HCl salt and mesylate, respectively, and the vehicle was 20% PEG400 in distilled water. Doses (10 mg/kg for **3**, 3 mg/kg for **19c** and **19d**) were body-weight-adjusted at the time of dosing. Compounds **3**, **19c**, and **19d** as test compounds and the vehicle as a control were orally administered once daily for 11 days. Tumor volumes (mg) and body weights (g) were recorded twice a week from all groups using a Vernier caliper and balance.

Acknowledgment. This study was supported by the Korea Ministry of Knowledge Economy (Grant No. 10016636), the Korea Science and Engineering Foundation (KOSEF), and the WCU program through KOSEF funded by the Korean Ministry of Education, Science, and Technology (MEST).

Supporting Information Available: ^{1}H NMR, ^{13}C NMR, and in vivo efficacy data for our leading compounds (**19c** and **19d**). This material is available free of charge via the Internet at http://pubs.acs.org.

References

(1) Schlessinger, J. Cell signaling by receptor tyrosine kinases. *Cell* **2000**, *103*, 211–225.
(2) Hynes, N. E.; Lane, H. A. ERBB receptors and cancer: the complexity of targeted inhibitors. *Nat. Rev. Cancer* **2005**, *5*, 341–354.
(3) Yarden, Y.; Sliwkowski, M. X. Untangling the ErbB signaling network. *Nat. Rev. Mol. Cell Biol.* **2001**, *2*, 127–137.
(4) Herbst, R. S.; Langer, C. J. Epidermal growth factor receptors as a target for cancer treatment: The emerging role of IMC-C225 in the treatment of lung and head and neck cancers. *Semin. Oncol.* **2002**, *29*, 27–36.
(5) Traxler, P.; Bold, G.; Buchdunger, E.; Caravatti, G.; Furet, P.; Manley, P.; O'Reilly, T.; Wood, J.; Zimmermann, J. Tyrosine kinase inhibitors: from rational design to clinical trials. *Med. Res. Rev.* **2001**, *21*, 499–512.
(6) (a) Adjei, A. A. Epidermal growth factor receptor tyrosine kinase inhibitors in cancer therapy. *Drugs Future* **2001**, *26*, 1087–1092. (b) Renhowe, P. A. Inhibitors of growth factor receptor kinase-dependent signaling pathways in anticancer chemotherapy-clinical progress. *Curr. Opin. Drug Discovery Dev.* **2002**, *5*, 214–224.
(7) Ranson, M.; Hammond, L. A.; Ferry, D.; Kris, M.; Tullo, A.; Murray, P. I.; Miller, V.; Averbuch, S.; Ochs, J.; Morris, C.; Feyereislova, A.; Swaisland, H.; Rowinsky, E. K. ZD1839, a selective oral epidermal growth factor receptor-tyrosine kinase inhibitor, is well tolerated and active in patients with solid, malignant tumors: results of a phase I trial. *J. Clin. Oncol.* **2002**, *20*, 2240–2250.
(8) Ciardiello, F.; Tortora, G. A novel approach in the treatment of cancer: Targeting the epidermal growth factor receptor. *Clin. Cancer Res.* **2001**, *7*, 2958–2970.
(9) Maheswaran, S.; Sequist, L. V.; Nagrath, S.; Ulkus, L.; Brannigan, B.; Inserra, E.; Diederichs, S. Detection of mutations in EGFR in circulating lung-cancer cells. *N. Engl. J. Med.* **2008**, *359*, 366–377.
(10) Wenle, X.; Mullin, R. J.; Keith, B. R.; Liu, L. H.; Ma, H.; Rusnak, D. W.; Owens, G.; Alligood, K. J.; Spector, N. L. Anti-tumor activity of GW-572016: A dual tyrosine kinase inhibitor blocks EGF activation of EGFR/erbB2 and downstream Erk1/2 and AKT pathways. *Oncogene* **2002**, *21*, 6255–6263.
(11) Johnston, S. R. D.; Leary, A. Lapatinib: A novel EGFR/HER2 tyrosine kinase inhibitor for cancer. *Drugs Today* **2006**, *42*, 441–453.
(12) (a) Tsou, H. R.; Overbeek-Klumpers, E. G.; Hallett, W. A.; Reich, M. F.; Floyd, M. B.; Johnson, B. D.; Michalak, R. S.; Shen, R.; Shi, X.; Wang, Y. F.; Upeslacis, J.; Wissner, A. Optimization of 6,7-disubstituted-4-(arylamino)quinoline-3-carbonitriles as orally active, irreversible inhibitors of human epidermal growth factor receptor-2 kinase activity. *J. Med. Chem.* **2005**, *48*, 1107–1131. (b) Rabindran, S. K.; Discafani, C. M.; Rosfjord, E. C.; Baxter, M.; Floyd, M. B.; Golas, J.; Hallett, W. A.; Johnson, B. D.; Nilakantan, R.; Overbeek, E.; Reigh, M. F.; Shen, R.; Shi, X.; Tsou, H. R.; Wang, Y. F.; Wissner, A. Antitumor activity of HKI-272, an orally active, irreversible inhibitor of the HER-2 tyrosine kinase. *Cancer Res.* **2004**, *64*, 3958–3965.
(13) Wissner, A.; Overbeek, E.; Reich, M. F.; Floyd, M. B.; Johnson, B. D.; Mamuya, N.; Rosfjord, E. C.; Discafani, C.; Davis, R.; Shi, X.; Rabindran, S. K.; Gruber, B. C.; Ye, F.; Hallett, W. A.; Nilakantan, R.; Shen, R.; Wang, Y.; Greenberger, L. M.; Tsou, H. Synthesis and structure−activity relationships of 6,7-disubstituted 4-anilinoquinoline-3-carbonitriles: The design of an orally active, irreversible inhibitor of the tyrosine kinase activity of the epidermal growth factor receptor (EGFR) and the human epidermal growth factor receptor-2 (HER-2). *J. Med. Chem.* **2003**, *46*, 49–63.
(14) (a) Smaill, J. B.; Showalter, H. D. H.; Zhou, H.; Bridges, A. J.; McNamara, D. J.; Fry, D. W.; Nelson, J. M.; Sherwood, V.; Vincent, P. W.; Roberts, B. J.; Elliott, W. L.; Denny, W. A. Tyrosine kinase inhibitors. 18. 6-Substituted 4-anilinoquinazolines and 4-anilinopyrido[3,4-*d*]pyrimidines as soluble, irreversible inhibitors of the epidermal growth factor receptor. *J. Med. Chem.* **2001**, *44*, 429–440. (b) Campos, S.; Hamid, O.; Seiden, M. V.; Oza, A.; Plante, M.; Potkul, R. K.; Lenehan, P. F.; Kaldjian, E. P.; Varterasian, M. L.; Jordan, C.; Charbonneau, C. Multicenter, randomized phase II trial of oral CI-1033 for previously treated advanced ovarian cancer. *J. Clin. Oncol.* **2005**, *23*, 5597–5604.
(15) Paez, J. G.; Janne, P. A.; Lee, J. C.; Tracy, S.; Greulich, H.; Gabriel, S.; Herman, P.; Kaye, F. J.; Lindeman, N.; Boggon, T. J.; Naoki, K.; Sasaki, H.; Fujii, Y.; Eck, M. J.; Sellers, W. R.; Johnson, B. E.; Meyerson, M. EGFR mutations in lung cancer: Correlation with clinical response to gefitinib therapy. *Science* **2004**, *304*, 1497–1500.
(16) Yun, C.; Mengwasser, K. E.; Toms, A. V.; Woo, M. S.; Greulich, H.; Wong, K.; Meyerson, M.; Eck, M. J. The T790M mutation in

EGFR kinase causes drug resistance by increasing the affinity for ATP. *Proc. Natl. Acad. Sci. U.S.A.* **2008**, *105*, 2070–2075.
(17) Kobayashi, S.; Boggon, T. J.; Dayaram, T.; Janne, P. A.; Kocher, O.; Meyerson, M.; Johnson, B. E.; Eck, M. J.; Tenen, D. G.; Halmos, B. EGFR mutation and resistance of non-small cell lung cancer to gefitinib. *N. Engl. J. Med.* **2005**, *352*, 786–792.
(18) Kobayashi, S.; Ji, H.; Yuza, Y.; Meyerson, M.; Wong, K. K.; Tenen, D. G.; Halmos, B. An alternative inhibitor overcomes resistance caused by a mutation of the epidermal growth factor receptor. *Cancer Res.* **2005**, *65*, 7096–7101.
(19) Engelman, J. A.; Zejnullahu, K.; Gale, C. M.; Lifshits, E.; Gonzales, A. J.; Shimamura, T.; Zhao, F.; Vincent, P. W.; Naumov, G. N.; Bradner, J. E.; Althaus, I. W.; Gandhi, L.; Shapiro, G. I.; Nelson, J. M.; Heymach, J. V.; Meyerson, M.; Wong, K. K.; Jänne, P. A. PF00299804, An irreversible pan-ERBB inhibitor, is effective in lung cancer models with *EGFR* and *ERBB2* mutations that are resistant to gefitinib. *Cancer Res.* **2007**, *67*, 11924–11932.
(20) Shintani, S.; Matsuo, K.; Crohin, C. C. Intragenic mutation analysis of the human epidermal growth factor receptor (EGFR) gene in malignant human oral keratinocytes. *Cancer Res.* **1999**, *59*, 4142–4147.
(21) Wildenhain, Y.; Pawson, T.; Blackstein, M. E.; Andrulis, I. L. p185neu is phosphorylated on tyrosine in human primary breast tumors which overexpress neu/erbB-2. *Oncogene* **1990**, *5*, 879–883.
(22) Kobayashi, S.; Ji, H.; Yuza, Y.; Meyerson, M.; Wong, K.; Tenen, D. G.; Halmos, B. An alternative inhibitor overcomes resistance caused by a mutation of the epidermal growth factor receptor. *Cancer Res.* **2005**, *65*, 7096–7101.
(23) Inhibition rate (%) = (1 − relative tumor growth in treated group/relative tumor growth in control group) × 100.
(24) (a) Lee, K.-O.; Gong, J. H.; Cha, M. Y.; Lee, C. G.; Kim, Y. H.; Lee, K.; Song, T. H.; Song, J. Y.; Park, Y.-J.; Kim, E. Y.; Lee, E.; Lee, K.; Kim, M. S.; Lee, G. S. Quinazoline derivatives for inhibiting the growth of cancer cell. PCT Int. Appl. WO2008002039A1, **2007**; (b) Ham, Y. J.; Gong, J. H.; Cha, M. Y.; Kim, J. W.; Kim, M. S.; Kim, E. Y.; Song, J. Y.; Kim, C. I.; Kim, S. Y.; Lee, G. S. Quinazoline derivatives for inhibiting cancer cell growth and method for the preparation thereof. PCT Int. Appl. WO2006071017A1, **2005**; (c) Gong, J. H.; Cha, M. Y.; Kim, J. W.; Lee, C. G.; Kim, S. Y.; Lee, K.-O.; Kim, M. S.; Kim, H. K.; Lim, C. K.; Kim, Y. H.; Lee, G. S. Quinazoline derivatives for inhibiting cancer cell growth and method for the preparation thereof. PCT Int. Appl. WO2006071079A1, **2005**.
(25) A431 cell washout test. A431 cells were incubated in 6-well plates to the extent of 500000 cells/well for 24 h. One set of cells were treated with 1 μM of **2** (Erlotinib) and the other set of cells were treated with 1 μM of analog **19c** for 4 h. Each set was washed four times with warmed compound-free medium and incubated for 8 h. Each set was simulated with EGF (100 ng/mL) for 5 min. The phosphorylation rate of EGFR was measured by Western blot. From this experiment, compound **19c** showed significant less phosphorylation rate (15%) of EGFR than **2** (100% phosphorylation). This result suggests that compound **19c** has an irreversible binding mode.
(26) $V = L \times S^2/2$ (V, tumor volume in milligrams; L, long diameter; S, short diameter).